



Contents lists available at ScienceDirect

## Journal of Human Evolution

journal homepage: [www.elsevier.com/locate/jhevol](http://www.elsevier.com/locate/jhevol)

## News and Views

## A re-evaluation of the taxonomic affinities of the early *Homo* cranium KNM-ER 42700

Karen L. Baab\*

Department of Anatomical Sciences, Stony Brook University, Stony Brook, NY 11794, USA

## ARTICLE INFO

## Article history:

Received 27 September 2007

Accepted 11 February 2008

Available online xxx

## Keywords:

Allometry

Cranial morphology

Cranial shape

Geometric morphometrics

*Homo erectus*

Spoor et al. (2007) described two recently discovered early *Homo* fossils from Ileret, Kenya. They allocated the small and relatively well-preserved calvaria KNM-ER 42700 to *Homo erectus*, while the partial maxilla (KNM-ER 42703) was attributed to *Homo habilis*. The taxonomic attribution of KNM-ER 42700 was based on a series of six cranial features and corroborated by a principal components analysis (PCA) of ten size-corrected cranial dimensions. It is necessary to carefully evaluate this taxonomic assessment because the presence of a small-sized African *H. erectus* at ~1.55 Ma has far-reaching implications for both the evolutionary history of *H. erectus* and its degree of sexual dimorphism.

Importantly, the inclusion of KNM-ER 42700 in *H. erectus* significantly expands the range of variation within this species, as it lacks several key diagnostic traits of *H. erectus* (e.g., a projecting supraorbital torus). Spoor et al. (2007) attributed the absence of certain features, including sagittal angulation of the occipital bone and low supraorbital thickness, to the presence of allometric scaling in early *Homo* based on a series of bivariate plots of several linear dimensions against endocranial volume.

Here I compare the shape of the KNM-ER 42700 cranium to *H. erectus* and other *Homo* taxa through PCA of three-dimensional (3D) neurocranial landmark data. Procrustes distances are then used to establish whether the differences observed between *H. erectus* and KNM-ER 42700 are most comparable to those seen in intra- or interspecific comparisons. Finally, I explore cranial allometry in *H. erectus* by incorporating information about both size

and shape into a single PCA (Mitteroecker et al., 2004) and then test whether the shape of KNM-ER 42700 fits predictions for an equivalently sized *H. erectus* cranium.

## Materials and methods

Cranial landmarks were collected from a representative sample of extant and fossil *Homo* specimens, including KNM-ER 42700 (Table 1). Missing bilateral landmarks were mirrored by reflecting their anteriors across the midline plane (reflected relabeling; Gunz and Harvati, 2006; McNulty et al., 2006). All specimens were then superimposed via generalized Procrustes analysis (GPA) so that the effects of scale, orientation, and translation were removed. Generalized Procrustes analysis works by superimposing specimens' centroids at a common origin, scaling configurations to a unit centroid size, and then rotating them until the residual sum-of-squares across all landmarks and specimens falls below a set tolerance level (Gower, 1975; Rohlf and Slice, 1990). The resulting configurations were then projected into linear tangent space for statistical analysis (Rohlf and Slice, 1990).

Two different landmark sets were used to explore the affinities of KNM-ER 42700 (Table 1; Fig. 1). A standard shape space PCA was performed on the first set of landmarks that were designed to approximate the endpoints of the cranial dimensions used by Spoor et al. (2007) in their PCA, as indicated in Table 2. The fossil sample associated with the first landmark set, while not identical to that analyzed by Spoor et al. (2007), was similarly representative of the size, geographic, and temporal ranges of this species ( $n = 16$ ). All statistical analyses were performed in Morphologika<sup>2</sup> (O'Higgins and Jones, 2006) and SAS 8.2 (SAS Institute, 1999–2001).

Two PCAs were performed on a second, more comprehensive set of landmarks. The first was a standard PCA in shape space. A more extensive hominin sample that included most *Homo* taxa ( $n = 67$ ) was used in order to place KNM-ER 42700 in a broader systematic context. To better understand the range of variation expected in a geographically widespread *Homo* species, this same data set was used to compare the range of Procrustes distances between KNM-ER 42700 and *H. erectus* to the distribution of distances within and between closely related *Homo* species. Procrustes distances (calculated using tpsSmall; Rohlf, 2003) are the distances among individuals in Kendall's shape space, the non-Euclidean shape space of specimens after GPA superimposition (Rohlf, 1999).

\* Tel.: +1 (631) 444 2618.

E-mail address: [baab@nycepc.org](mailto:baab@nycepc.org)

**Table 1**  
Landmarks and specimens used in principal components analyses

Landmarks <sup>a</sup>	Sample	
	Taxon	Specimens
<b>First landmark set</b>		
Opisthion, inion, opisthocranion, lambda, apex, bregma, glabella, asterion, parietal notch, porion, lateral articular fossa, inferior entoglenoid	Unknown	KNM-ER 42700
	<i>H. habilis</i>	KNM-ER 1813
	<i>H. erectus</i>	KNM-ER 3733, 3883; Daka; D2280, <sup>b</sup> 2700 <sup>b</sup> ; S 17 <sup>b</sup> ; Ng 6, 11, 12; Ngawi <sup>b</sup> ; Zkd 3, <sup>b</sup> 11, <sup>b</sup> 12 <sup>b</sup>
<b>Second landmark set</b>		
Opisthion, inion, lambda, mid-parietal, bregma, <sup>c</sup> midline post-toral sulcus, glabella, anterior pterion, mid-temporal squama, porion, auriculare, temporosphenoid suture, parietal notch, asterion, tympanomastoid fissure, postglenoid, inferior entoglenoid, mid-torus inferior, mid-torus superior, frontotemporale, frontomale temporale, frontomale orbitale	Unknown	KNM-ER 42700
	<i>H. habilis</i>	KNM-ER 1813
	<i>H. erectus</i>	KNM-ER 3733, 3883; Daka; D2280, <sup>b</sup> 2700, <sup>b</sup> 3444 <sup>b</sup> ; S 17 <sup>b</sup> ; Ng 6, 11, 12; Sm 3; Zkd 11, <sup>b</sup> 12 <sup>b</sup>
	Middle Pleistocene <i>Homo</i>	Kabwe, Dali <sup>b</sup>
	Neanderthals	La Chapelle, <sup>b</sup> La Ferrassie <sup>b</sup>
Early <i>H. sapiens</i>	Skhul 5	
Recent <i>H. sapiens</i>	Fish Hoek, Abri Pataud, <sup>b</sup> Liujiang <sup>b</sup> (Upper Paleolithic) and 43 individuals from 11 geographically dispersed groups <sup>d</sup>	

<sup>a</sup> Definitions can be found in Baab (2007).

<sup>b</sup> Casts were used.

<sup>c</sup> In KNM-ER 42700, bregma was recorded a few millimeters anterior to the broken edge of, but in line with, the parietal bones, as the frontal bone appeared to be shifted inferiorly at the coronal suture.

<sup>d</sup> Details regarding the modern human sample can be found in Baab (2007).

The final PCA utilized this second (more complete) set of landmarks and the logarithm of centroid size (log CS), shifting the analysis from shape space to form space (size-shape space). Centroid size is defined as the square root of the sum of squared distances from each landmark to the centroid and can be viewed as a multivariate proxy for the overall size of each specimen. Mitteroecker et al. (2004) first introduced PCA in form space to explore cranial ontogeny in humans and great apes. Due to the great variability in log CS relative to the other variables, the first PC will be closely related to size differences. As described below, linear-regression analysis showed a significant relationship between log CS and scores for the first two principal components (PC 1 and 2) within adult *H. erectus*. These regressions were then used to predict where a *H. erectus* cranium the same size as KNM-ER 42700 would plot on these two components. To assess whether the shape of its cranium was within expectations for a small *H. erectus* individual, the observed position of KNM-ER 42700 was then compared to this prediction.

To reinforce the results of the form space analysis, multivariate regressions of all shape variables on log CS were used to predict the shape of a hypothetical specimen the same size as KNM-ER 42700. The advantage of this approach is that it uses all shape variation correlated with size rather than just the variation captured on PCs 1 and 2. The form space PCA was then re-run with this simulated landmark configuration. While the positions of individual specimens along PCs 1 and 2 were not identical to the original form space PCA, the results were not qualitatively different. The position

of the simulated specimen in the original form space PCA was therefore approximated based on these results.

## Results

The KNM-ER 42700 cranium falls outside of the 95% prediction confidence ellipse and the convex hull for *H. erectus* in the standard PCAs of both landmark sets (Fig. 2). In the PCA of the first landmark set (corresponding to the endpoints of the measurements taken by Spoor et al., 2007), KNM-ER 42700 is well separated from both *H. erectus* and *H. habilis* along PC 1, plotting closest to the Daka specimen and D3444 from Dmanisi (Fig. 2a). The two East Turkana fossils closest in age to KNM-ER 42700 (KNM-ER 3733 and KNM-ER 3883) score much lower on the first component. Higher scoring individuals on PC 1, including KNM-ER 42700, have a more superiorly positioned opisthocranion, greater posterior expansion of the lambdoidal region, a higher cranial vault at bregma/apex, a more inferiorly positioned parietomastoid suture, a more anteriorly located opisthion, and less laterally positioned poria.

Differences in size account for some of the variation in PC 2 scores ( $p = 0.0011$ ,  $r^2 = 0.54$ ), a relationship that is even stronger when KNM-ER 42700 is excluded ( $p = 0.0002$ ,  $r^2 = 0.67$ ). The small Dmanisi fossils score lowest, in contrast to the larger Asian specimens on this component. If KNM-ER 42700 is a representative of *H. erectus*, then it scores higher than expected given its small size. Although not shown, PC 3 highlights the unique shape of the

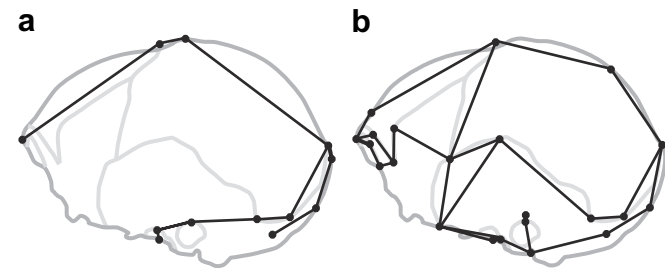


**Fig. 1.** Landmarks illustrated on line drawings of KNM-ER 42700: (a) the first landmark set reflects the linear measurements used by Spoor et al. (2007) in their PCA, while (b) the second landmark set better reflects the overall shape of the neurocranium. The wireframe connecting the landmarks is for visualization purposes only.

**Table 2**  
Correspondence between the linear measurements used by Spoor et al. (2007) and the landmarks used in the first PCA

Spoor et al. measurement	Landmarks <sup>a</sup> from first landmark set
Maximum length	Glabella–opisthocranion
Porion–vertex height	Porion–apex
Maximum breadth	Parietal notch (right)–parietal notch (left) <sup>b</sup>
Glabella–bregma chord	Glabella–bregma
Parietal sagittal chord	Bregma–lambda
Lambda–inion chord	Lambda–inion
Inion–opisthion chord	Inion–opisthion
Occipital sagittal chord	Lambda–opisthion
Bi-asterionic breadth	Asterion (right)–asterion (left)
Mandibular fossa breadth	Inferior entoglenoid–lateral articular fossa

<sup>a</sup> Landmark definitions can be found in Baab (2007).

<sup>b</sup> The parietal notch landmarks were used to approximate the maximum breadth of the cranium because maximum cranial breadth in archaic *Homo* is located across the temporal squamae (Rightmire, 1990).

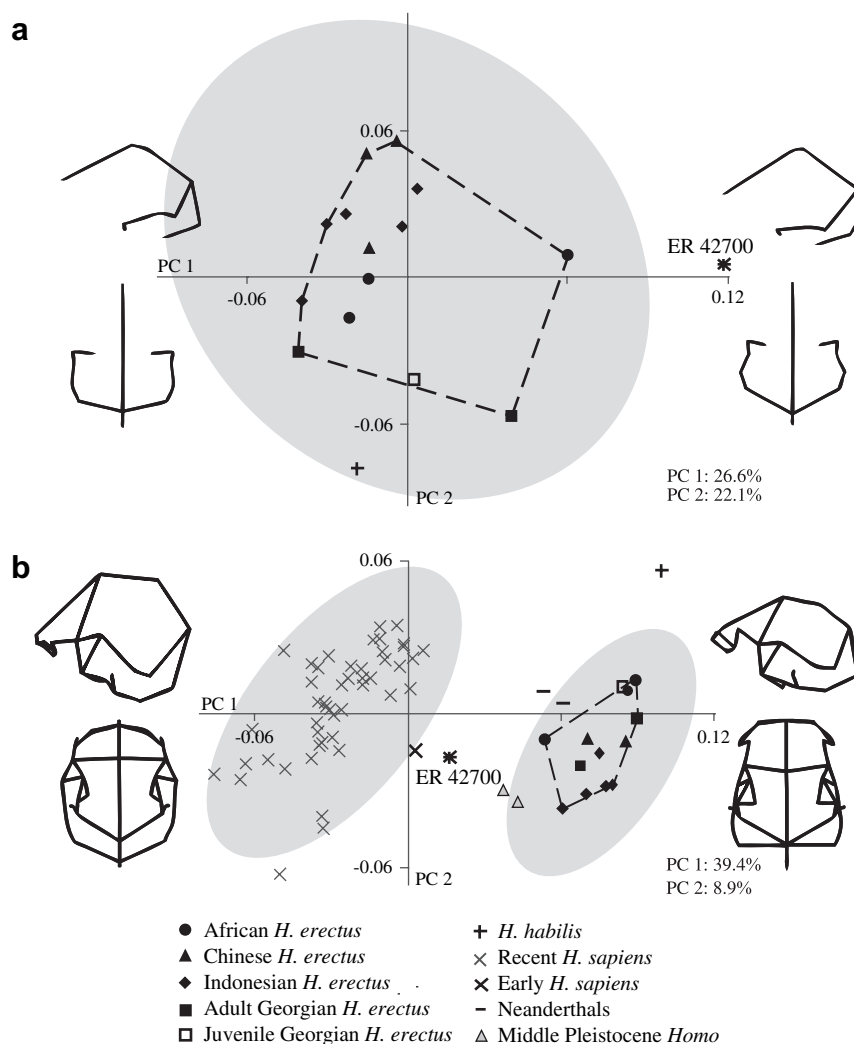


**Fig. 2.** Ordinations of PC 1 vs. PC 2 for (a) the landmarks that correspond to the endpoints of the measurements used by Spoor et al. (2007) and (b) the more comprehensive set of calvarial landmarks. The dashed line represents the convex hull (minimum polygon that includes all specimens) for *H. erectus*, while the shaded regions are the 95% confidence prediction ellipses for *H. erectus* and *H. sapiens*. In both cases, KNM-ER 42700 falls well outside of both the convex hull and the 95% ellipse for *H. erectus*. The shape associated with the positive and negative ends of PC 1 are shown in left lateral and superior views. Wireframes correspond to Fig. 2.

Javanese *H. erectus* crania; KNM-ER 42700 plotted toward the center of this component. Clear patterns were not identified on subsequent PCs.

In the second PCA (which included more landmarks and more specimens; Fig. 2b), the first component reads, from right to left, as a rough archaic-to-modern distribution. Within this context, the shape of the KNM-ER 42700 calvaria is more modern in appearance than that of other *H. erectus* and even more so than Middle Pleistocene *Homo* (Kabwe and Dali) and the Neanderthals. This result is due to the greater posterosuperior expansion of the posterior vault, steeper frontal squama, greater width across the frontal and temporal squamae, reduced postorbital constriction (i.e., greater bi-frontotemporale breadth relative to cranial breadth), and thinner supraorbital elements.

Within *H. erectus*, Daka and Sm 3 have the next lowest scores on PC 1. That Daka has a more expanded vault relative to other African *H. erectus* (lowest scoring *H. erectus* fossil on PC 1) is not surprising given the younger age of this specimen (~1 Ma; Asfaw et al., 2002). The Sm 3 specimen has the next lowest score of all the *H. erectus* fossils, which fits with previous descriptions of this cranium as shorter and higher than other contemporary Javanese *H. erectus* (Delson et al., 2001). The relatively anteroposteriorly shorter and superoinferiorly taller neurocranium of KNM-ER

42700 is less easy to interpret in this context, as this specimen is 1.55 Ma, more than 500 kyr older than Daka and perhaps 1.0–1.5 Myr older than Sm 3 (Swisher et al., 1996). With the exception of D3444, all other Dmanisi and East Turkana fossils are the highest scoring *H. erectus* fossils on PC 1. The higher score of D3444 is still well within the range of *H. erectus*. In general, the position of KNM-ER 42700 in the PC plot does not appear to be related to its small size, as the relationship between size and PC 1 or 2 scores is not significant.

Subsequent PCs each accounted for less than 6% of the total variance and most did not demonstrate clear taxonomic, geographic, or allometric patterns. The third PC contrasted shorter, wider neurocrania (e.g., Daka and Sm 3) to longer, narrower ones (e.g., Ng 6 and Zkd 11); KNM-ER 42700 plotted in an intermediate position along this component. Of the first ten PCs, size of the *H. erectus* adult crania was significantly related to the scores on PCs 4 and 5 only, and in neither case did KNM-ER 42700 fall along the *H. erectus* allometric trajectory.

Intra- and interspecific Procrustes distances were calculated based on the second landmark set and are summarized in Fig. 3. The range of distances from KNM-ER 42700 to each *H. erectus* fossil more closely resembles the interspecific ranges than the intraspecific ranges. Although there was overlap in the absolute

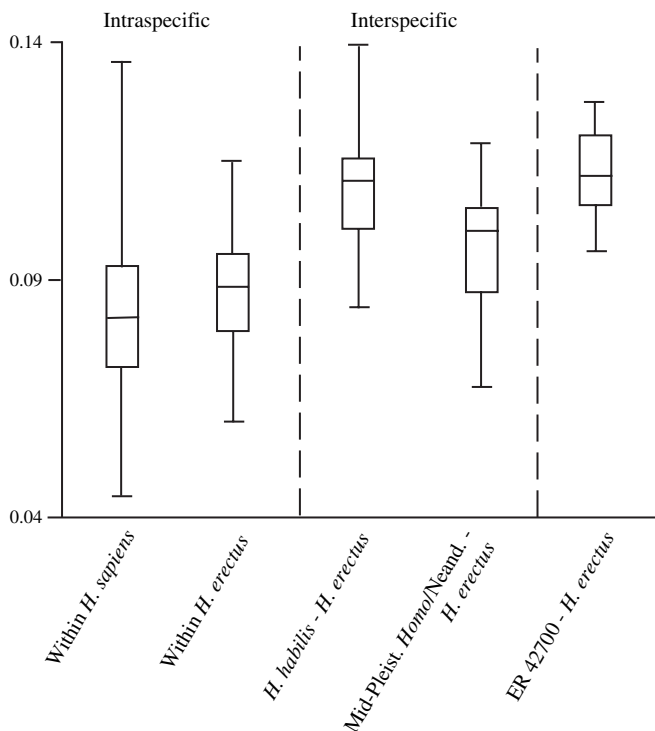


**Fig. 3.** Comparison of intraspecific and interspecific ranges of Procrustes distances within *Homo* to the distances observed between KNM-ER 42700 and *H. erectus*. Distances are based on the second landmark set. The box plots illustrate the median value, first and third quartiles, and extreme values.

ranges of Procrustes distances, the medians for the intra- and interspecific comparisons were well separated. The median Procrustes distance for KNM-ER 42700–*H. erectus* (0.113) was slightly higher than the values for both the Middle Pleistocene *Homo*/Neanderthal–*H. erectus* and *H. habilis*–*H. erectus* comparisons (0.100 and 0.111, respectively) and well above the median intraspecific values of 0.082 (within *H. sapiens*) and 0.088 (within *H. erectus*).

A second PCA of the more complete landmark set was conducted in form space to evaluate patterns of cranial allometry (Fig. 4). As expected, the first PC is closely tied to size variation (regression of PC 1 scores on log CS:  $r^2 = 0.96$ ,  $p < 0.0001$ ), but it also reflects those aspects of shape variation that are correlated with size across taxa. Shape differences among the taxa, particularly between modern humans and early *Homo*, are captured by the second component. There is also a relationship between PC 2 scores and size within *H. erectus* ( $r^2 = 0.72$ ,  $p = 0.0005$ ), and thus the structure evident in the PC plot reflects allometric scaling within this species.

The regression of PC 1 and 2 scores of adult *H. erectus* on log CS were used to predict the corresponding scores for a specimen the size of KNM-ER 42700 (Fig. 4a). The KNM-ER 42700 cranium falls just outside of this 95% prediction interval for PC 1 and well outside the range for PC 2, suggesting that its shape is not within expectations for a comparably sized *H. erectus* cranium. Using the same method, prediction intervals were calculated for a specimen the size of D2700, a small subadult cranium from Dmanisi. This specimen falls within these 95% prediction intervals for both PC 1 and 2. A simulated specimen identical in size to KNM-ER 42700 was generated based on all shape variation correlated with size (target in Fig. 4a). This hypothetical specimen falls in the prediction interval generated for a specimen the size of KNM-ER 42700, confirming that PC 1 and 2 reflect relevant allometric patterns in *H. erectus*.

The changes in cranial shape corresponding to size differences are shown in Fig. 4 (b, c). Although KNM-ER 42700 follows some of the broad allometric trends present in *H. erectus*, they were generally taken to a greater extreme than predicted for the size of this cranium. As seen in Fig. 4d, the KNM-ER 42700 calvaria has a taller midsagittal contour, a more posterosuperiorly angled upper occipital scale, a thinner supraorbital torus, a narrower mandibular fossa, and wider frontal and temporal squamae than predicted for a comparably sized *H. erectus* specimen based on these allometric trajectories.

## Discussion and conclusions

The results of the standard (shape space) PCAs contrast with the multivariate analysis of linear measurements presented by Spoor et al. (2007). While multivariate analysis of both linear measurements and 3D landmark data share the same goal of approximating shape, the first PCA presented here (Fig. 2) demonstrates that these approaches are not always equivalent. The latter approach has the advantage of retaining the original geometry of the specimens (Rohlf and Marcus, 1993; O'Higgins, 2000; Adams et al., 2004), and it indicates that the actual shape of the KNM-ER 42700 calvaria is quite distinct from that of other *H. erectus* specimens.

*Homo erectus* is among the most extensively sampled fossil hominin species, suggesting that the range of variation (at least in the crania) is well documented. This is particularly true for cranial size, as the endocranial volume of Ngandong 6 is about twice that recorded for D2700 (1251 cm<sup>3</sup> vs. ~612 cm<sup>3</sup>; Holloway, 1980; Rightmire et al., 2006). Yet, the relatively wider and more posteriorly expanded vault, decreased constriction across fronto-temporale, and steeper frontal squama with thinner supraorbital elements seen in KNM-ER 42700 is well outside the documented range of variation for this species (Fig. 2). Spoor et al. (2007) described KNM-ER 42700 as an older subadult or young adult individual based on the spheno-occipital synchondrosis, which is mostly, but not entirely, fused. Although the possible subadult status and small size of this fossil complicate interpretations of its cranial morphology, the similarly small Dmanisi fossils, including the developmentally younger D2700 (based on fusion of the spheno-occipital synchondrosis), bear greater similarity to other *H. erectus* fossils in their cranial morphology (Figs. 2 and 4; Rightmire et al., 2006).

Although certain aspects of cranial shape are consistent across the *H. erectus* hypodigm, cranial morphology is not homogeneous within the species (Rightmire, 1990; Bilsborough, 2000; Antón, 2002, 2003; Asfaw et al., 2002). Rather, intraspecific differences in cranial shape are influenced by chronologic, geographic, and allometric variation within *H. erectus* (Baab, 2007). In this context, the morphology of the KNM-ER 42700 cranium does not conform to the broad patterns of intraspecific variation documented for this species, as it is particularly distinct relative to other early, small *H. erectus* fossils from Africa and Eurasia (i.e., Dmanisi). Additionally, the differences between KNM-ER 42700 and *H. erectus* are more comparable to those seen in interspecific comparisons within the genus *Homo* (Fig. 3).

While additional variation almost certainly remains to be documented for *H. erectus*, it is difficult to imagine that the allometric trajectory described here for this species would change in such a way as to incorporate KNM-ER 42700. The deviation of this specimen from the common allometric pattern is perhaps the most convincing evidence that the taxonomic attribution of this fossil needs to be further evaluated. It follows that the lack of certain diagnostic *H. erectus* features cannot be attributed to allometric scaling in this species, as suggested by Spoor et al. (2007).

Unfortunately, inadequate preservation of early non-*erectus* *Homo* specimens (e.g., KNM-ER 1470, KNM-ER 1805, OH 13, OH 16,

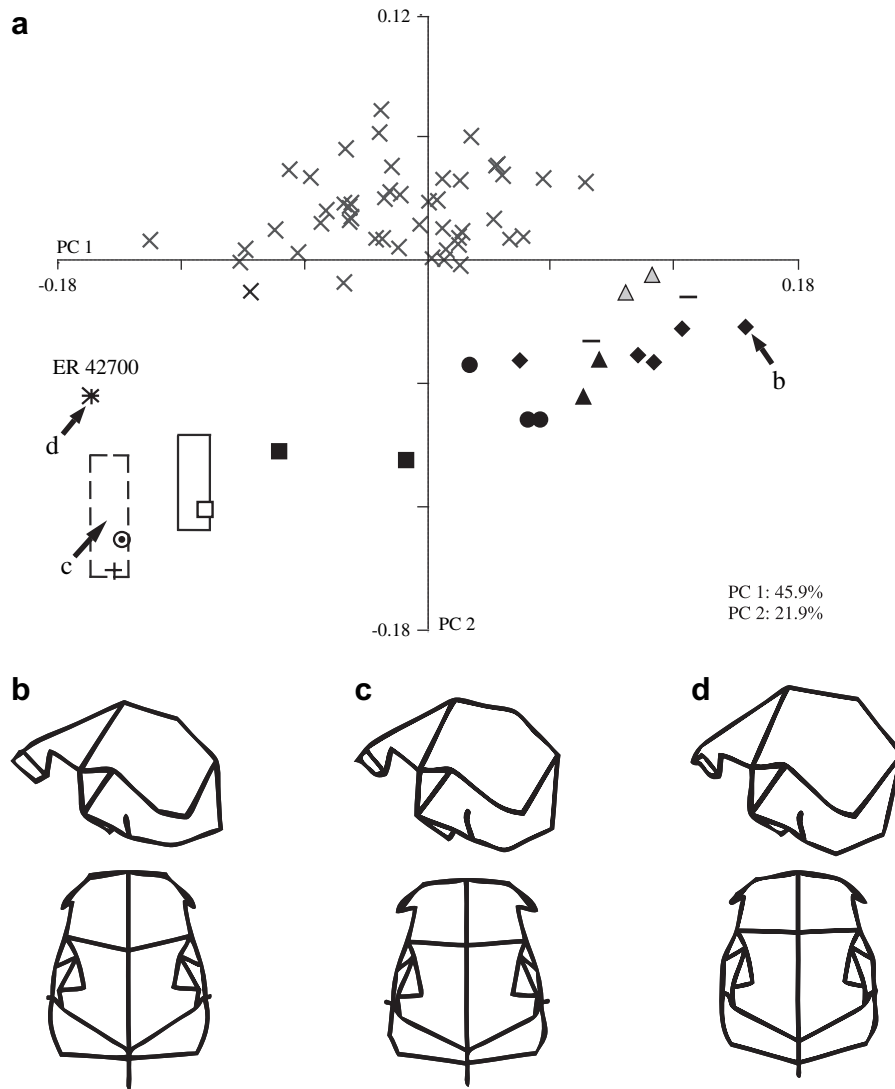


**Fig. 4.** (a) PCA of shape coordinates from second landmark set plus the log of centroid size. Smaller specimens score lower on PC 1 and larger specimens have higher scores on this component. The rectangle formed by the dashed line is the 95% prediction interval along PCs 1 and 2 for a specimen the size of KNM-ER 42700 based on adult *H. erectus*, whereas the rectangle formed by the solid line indicates the prediction interval for a specimen the size of D2700. Specimen KNM-ER 42700 falls just outside the predicted range for PC 1 and well outside the interval for PC 2. Specimen D2700 falls within its associated prediction interval for the first two components. The shape associated with (b) large *H. erectus* fossils, (c) the predicted position for KNM-ER 42700, and (d) the actual position of KNM-ER 42700 are illustrated in left lateral and superior views. Symbols are as in Fig. 2; the approximate position of a simulated specimen the same size as KNM-ER 42700 based on all shape variation correlated with size in *H. erectus* is indicated by the target (⊙).

and Stw 53) limits the comparisons between KNM-ER 42700 and other contemporaneous *Homo* species in this study, leaving its taxonomic position uncertain. Nevertheless, the questionable inclusion of KNM-ER 42700 in *H. erectus* could mask potentially important variation in the early Pleistocene hominin record of Africa and confuse interpretations of sexual dimorphism in early *H. erectus* (Spoor et al., 2007). Although future discoveries may fill in the morphological gap between this specimen and other early/small *H. erectus* fossils, until then it is preferable to assign KNM-ER 42700 to *Homo* sp. in order to emphasize the uniqueness of this fossil's morphological pattern.

#### Acknowledgements

I am grateful to R. Raab, E. Delson, and W. Jungers for helpful comments on earlier drafts of this manuscript. I offer my sincerest appreciation to F. Spoor, M. Leakey, S. Antón and colleagues for their permission to study KNM-ER 42700 prior to their initial publication. I am indebted to W. Kimbel, D. Lieberman, F. Spoor, and two

anonymous reviewers for reviewing and commenting on this manuscript. I also acknowledge the curators and staff of the following institutions: American Museum of Natural History, Aristotle University of Thessaloniki, Duckworth Collection at the University of Cambridge, Gadjra Mada University, LIPI, Musée de L'Homme, National Museums of Ethiopia, National Museums of Kenya, National Museum of Tanzania, COSTECH, Natural History Museum, Peabody Museum at Harvard University, University of Cape Town, and the Institut de Paleontologie Humaine for allowing us access to fossil and comparative samples. Grant support was provided by NSF (BCS 04-24262, DGE 03-33415, and DBI 96-02234), the L.S.B. Leakey Foundation, and the Sigma Xi Foundation. This is NYCEP Morphometrics contribution 29.

#### References

- Adams, D.C., Rohlf, F.J., Slice, D.E., 2004. Geometric morphometrics: ten years of progress following the 'revolution.' *Ital. J. Zool.* 71, 5–16.
- Antón, S.C., 2002. Evolutionary significance of cranial variation in Asian *Homo erectus*. *Am. J. Phys. Anthropol.* 118, 801–828.

- Antón, S.C., 2003. Natural history of *Homo erectus*. Yearb. Phys. Anthropol. 46, 126–170.
- Asfaw, B., Gilbert, W.H., Beyene, Y., Hart, W.K., Renne, P.R., WoldeGabriel, G., Vrba, E. S., White, T.D., 2002. Remains of *Homo erectus* from Bouri, Middle Awash, Ethiopia. Nature 416, 317–320.
- Baab, K.L., 2007. Cranial shape variation in *Homo erectus*. Ph.D. Dissertation, City University of New York.
- Bilsborough, A., 2000. Chronology, variability and evolution in *Homo erectus*. Var. Evol. 8, 5–30.
- Delson, E., Harvati, K., Reddy, D., Marcus, L.F., Mowbray, K., Sawyer, G.J., Jacob, T., Marquez, S., 2001. The Sambungmacan 3 *Homo erectus* calvaria: a comparative morphometric and morphological analysis. Anat. Rec. 262, 380–397.
- Gower, J.C., 1975. Generalized Procrustes analysis. Psychometrika 40, 33–51.
- Gunz, P., Harvati, K., 2006. The Neanderthal “chignon”: variation, integration, and homology. J. Hum. Evol. 52, 262–274.
- Holloway, R.L., 1980. Indonesian “Solo” (Ngandong) endocranial reconstructions: some preliminary observations and comparisons with Neandertal and *Homo erectus* groups. Am. J. Phys. Anthropol. 53, 285–295.
- McNulty, K.P., Frost, S.R., Strait, D.S., 2006. Examining affinities of the Taung child by developmental simulation. J. Hum. Evol. 51, 274–296.
- Mitteroecker, P., Gunz, P., Bernhard, M., Schaefer, K., Bookstein, F.L., 2004. Comparison of cranial ontogenetic trajectories among great apes and humans. J. Hum. Evol. 46, 679–698.
- O’Higgins, P., 2000. The study of morphological variation in the hominid fossil record: biology, landmarks and geometry. J. Anat. 197, 103–120.
- O’Higgins, P., Jones, N., 2006. Morphologika<sup>2</sup>, v. 2.4. Hull York Medical School, York.
- Rightmire, G.P., 1990. The Evolution of *Homo erectus*: Comparative Anatomical Studies of an Extinct Human Species. Cambridge University Press, New York.
- Rightmire, G.P., Lordkipanidze, D., Vekua, A., 2006. Anatomical descriptions, comparative studies and evolutionary significance of the hominin skulls from Dmanisi, Republic of Georgia. J. Hum. Evol. 50, 115–141.
- Rohlf, F.J., 1999. Shape statistics: Procrustes superimpositions and tangent spaces. J. Classif. 16, 197–223.
- Rohlf, F.J., 2003. tpsSmall, v. 1.20. Ecology and Evolution. State University of New York, Stony Brook.
- Rohlf, F.J., Marcus, L.F., 1993. A revolution in morphometrics. Trends Ecol. Evol. 8, 129–132.
- Rohlf, F.J., Slice, D., 1990. Extensions of the Procrustes method for the optimal superimposition of landmarks. Syst. Zool. 39, 40–59.
- Spoor, F., Leakey, M.G., Gathogo, P.N., Brown, F.H., Antón, S.C., McDougall, I., Kiarie, C., Manthi, F.K., Leakey, L.N., 2007. Implications of new early *Homo* fossils from Ileret, east of Lake Turkana, Kenya. Nature 448, 688–691.
- Swisher III, C.C., Rink, W.J., Antón, S.C., Schwarcz, H.P., Curtis, G.H., Suprijo, A., Widiasmoro, 1996. Latest *Homo erectus* of Java: potential contemporaneity with *Homo sapiens*. Science 274, 1870–1874.